mathematics

MDPI

Article

Exact Solutions of the Bloch Equations to the Asymmetric Hyperbolic Cosine Pulse with Chirped Frequency

Sofiane Grira [1,*], Nadia Boutabba [2] and Hichem Eleuch [3,4]

[1] Department of Mathematics and Statistics, Abu Dhabi University, Abu Dhabi 59911, United Arab Emirates
[2] Institute of Applied Technology, Fatima College of Health Sciences, Abu Dhabi 24162, United Arab Emirates
[3] Department of Applied Physics and Astronomy, College of Sciences, University of Sharjah, Sharjah 27272, United Arab Emirates
[4] Institute for Quantum Science and Engineering, Texas A&M University, College Station, TX 77843, USA
* Correspondence: grira.sofiane@adu.ac.ae

Abstract: In this research study, we derive the exact solutions of the Bloch equations describing the dynamics of a two-level atom with dephasing. In the two-level atom, a strong laser pump couples a ground state to an upper excited state with a time-dependent Rabi-frequency. The exact solutions are given for the atomic population inversion and the real and imaginary parts of the coherence while the input pulse is an asymmetric hyperbolic cosine form. Additionally, the system is under a chirped detuning. The method of solving the Bloch equations analytically is a very tedious part of the research, and as far as we know, there are few exact solutions available in this field. Hence, our solutions might be of great interest to various research areas, including nuclear magnetic resonance, where analytical solutions to the Bloch equations play a major role in the study of the information on the state of the medium as determined by the NMR signals.

Keywords: atomic population control; two-level atom; exact solutions

MSC: 81-10; 81V45; 81V80

Citation: Grira, S.; Boutabba, N.; Eleuch, H. Exact Solutions of the Bloch Equations to the Asymmetric Hyperbolic Cosine Pulse with Chirped Frequency. *Mathematics* **2023**, *11*, 2159. https://doi.org/10.3390/math11092159

Academic Editors: Dmitry Makarov and Davide Valenti

Received: 24 February 2023
Revised: 21 April 2023
Accepted: 28 April 2023
Published: 4 May 2023

1. Introduction

The Bloch equations, named after Felix Bloch in 1946 [1], provide exceptional insights into many processes, not only in optics [2–11] but also in nuclear magnetic resonance research [12–15]. In the field of optics, they are referred to as the optical Maxwell Bloch equations and they describe the quantum dynamics of a multi-level atom interacting with electromagnetic fields [16–20]. However, these equations can be difficult or impossible to solve analytically. Hence, the solutions are usually limited to the two-level atom and under some specific excitation shape pulses. Nonetheless, such systems constitute the basic framework of many processes that are modeled and comprehended by the two-level approximation. Zlatanov et al. [21], derived the "exact solution of the Bloch equations for the non-resonant exponential model in the presence of dephasing". The equations were reduced to the Demkov model, and the solution was expressed in terms of the generalized hypergeometric function. Exact solutions of a two-level atom pumped by generalized double exponential quotient pulses with dephasing were also obtained in [22]. Furthermore, Boutabba et al. [23] studied the excitation of a multi-level atomic system using a fast laser pulse with a q-deformed hyperbolic waveform. Hence, the authors first derived the exact solution to the Bloch equations describing a two-level atom with dephasing and time-dependent detuning. Next, they investigated the probe field's absorption and dispersion properties, as well as the coherence's dependence on the q-deformation of the Rb^{87} atomic system. To obtain an analytical solution, Zhang et al. solved the Bloch equation pumped by a hyperbolic-secant pulse in the field of medical magnetic resonance [24]. Additionally, Silver et al obtained the analytical solution of the Bloch equation by solving

the Bloch–Riccatti and by considering the case of an initial magnetization parallel to the z-axis [25].

The optical Bloch equations for the Demkov model were investigated in [26] and the exact solutions were derived for the coherent resonant case of a two-level quantum system excited by a time-dependent external field in the presence of dephasing. Moreover, by deriving the coherence components of the Bloch vector, the authors explained the mechanism by which the population transfer is blocked.

In this paper, we solve the Bloch equations describing a two-level atom excited by a shaped laser waveform and chirped detuning. These kinds of shaped waveforms are very efficient in the realization of the atomic population inversion and are widely used in the field of digital communications. For instance, a shaped waveform with the mathematical description of a Tan-hyperbolic is used as sudden switching on–off RF-pulse generator [27]. In addition, it is worth noting that, the CPA laser technique (chirped population amplification) makes extensive use of chirping pulses to create ultra-short, extremely high-energy lasers [28–33]. These pulses are effective in implementing atomic population transfers in molecules and atoms. This manuscript is structured as follows: in Section 2 we present the model, then we describe our technique, followed by the analytical solutions of the Bloch equations where we derive the real and the imaginary part of the coherence, as well as determining the full exact solution of the atomic population inversion in Sections 3 and 4. The pulse derived in the current research work is given by the generalized q-deformed hyperbolic cosine pulse exciting a two-level atom with a chirped frequency.

2. Model

Our model is based on the classical scheme of the two-level atom pumped by an external time-dependent field [17,34,35]. Such systems serve as a basic framework to illustrate pertinent light phenomena in atomic systems such as the absorption and the fluorescence spectra of light, the coherent control of quantum systems, and other quantum information processes (quantum bits, supraconductor quantum circuits, and squeezing of light) [36,37]. The two-level atom is usually excited from the ground state to an upper state with an external field that has a transition frequency ω so that, ω=ω_2-ω_1 and ω_1 and ω_2 are, respectively, the frequencies of the atom at states $|1\rangle$ and $|2\rangle$ (See Figure 1). In this situation, we describe the Hamiltonian [21,38,39] in the interaction picture under the rotating wave approximation by using the Pauli matrices σ_x, and σ_z and by considering the time-dependent Rabi frequency $\Omega(t)$:

$$H = \frac{\hbar}{2}(\Delta(t)\sigma_z + \Omega(t)\sigma_x) \tag{1}$$

The Rabi frequency is related to the amplitude of the laser pulse as:

$$\Omega(t) = -d\frac{E(t)}{\hbar} \tag{2}$$

d is the dipole moment, $\Delta = \omega_2 - \omega_1$ is the chirped detuning. The density matrix describes the evolution of the system:

$$\frac{d\rho(t)}{dt} = -i[H, \rho] + \frac{\Gamma}{2}(\sigma_z\rho\sigma_z - \rho) \tag{3}$$

The above equation is the Lindblad Equation of a two-level atomic system. In general, the Lindblad equation describes the dynamics of the Markovian Master equation which governs the coupling between a quantum system and its environment. The first term illustrates the Liouville-von Neumann equation, which is linked to the unitary evolution of the density operator. The last term of Equation (3) (the Lindblad operator) represents the interaction with the environment which is related to the non-unitary evolution of the density operator. The Lindblad operator typically expresses the different ways in which

the environment can affect the system including dephasing, dissipation, and relaxation. Although dephasing, relaxation, and dissipation are separate processes, they can all take place at the same time in an open quantum system and are all explicable within the same framework of the Lindblad equation. All these processes can be expressed in the Lindblad operator, which describes the coupling between the quantum system and its surroundings. Here, we focus on the effect of dephasing, a process involving the loss of coherence in the quantum system due to its interaction with the environment, since it is crucial in several physical systems, particularly in quantum computing and quantum information processing. Dephasing in these systems has the potential to impair the performance of quantum devices by causing errors in computation or information storage. Therefore, one of the key areas of research in the field of quantum information science is understanding and minimizing the loss of coherence effects. Therefore, Γ in Equation (3) can be interpreted as the dephasing rate inversely proportional to the dephasing time.

Our purpose in the current study, is to establish exact analytical solutions of the density matrix elements, then derive the atomic population inversion $w = \rho_{22} - \rho_{11}$ at the steady state ($t = \infty$).

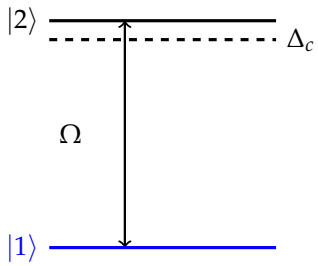

Figure 1. Two-level atom.

The Bloch equations are given by:

$$\begin{bmatrix} \frac{du(t)}{dt} \\ \frac{dv(t)}{dt} \\ \frac{dw(t)}{dt} \end{bmatrix} = \begin{bmatrix} -\Gamma & -\Delta(t) & 0 \\ \Delta(t) & -\Gamma & -\Omega(t) \\ 0 & \Omega(t) & 0 \end{bmatrix} \begin{bmatrix} u(t) \\ v(t) \\ w(t) \end{bmatrix} \tag{4}$$

Here, the atomic population inversion between the higher state $|2\rangle$ and the ground state $|1\rangle$ is denoted by $w = \rho_{22} - \rho_{11}$,whereas $u(t)$ and $v(t)$ represent the real and the imaginary part of the atom–field coherence $2\rho_{12}(t)$.

3. The Exact Solutions: Method

This section's objective is to develop precise analytical solutions for the atomic population and the coherence of the following optical pulse form:

$$\Omega = A_1 e^{-3\Gamma t}(1 + Ke^{-2\Gamma t}) \tag{5}$$

under chirped detuning of the form:

$$\Delta = A_2 e^{-2\Gamma t}(1 + Ke^{-2\Gamma t}) \tag{6}$$

where $A_1 = -8\Gamma K$, $A_2 = -8\Gamma K^{\frac{3}{2}}$ are negative constants and $K > 0$. It is worth noting that the considered optical pulse is a combination of two exponential pulses. These types of pulses and their combinations are applied in [40,41]. The implementation of half-cycle pulses is realized in [42,43]. Such half-cycle pulses are similar to the EMG waveforms (Exponentially Modified Gaussians). A pertinent example was performed by D.J. Morrow et al. [44], where the authors used a summation of exponentially modified Gaussians to analyze time-resolved fluorescence data.

Using the generalized q-deformed hyperbolic cosine, which is defined by [45]:

$$\cosh_{(q,s)} x = \frac{e^x + qe^{-sx}}{2} \tag{7}$$

the exact solutions for the Bloch equations are derived for the asymmetric hyperbolic pulse for $s = -\frac{5}{3}$, then the pulses can be expressed as follows

$$\Omega = 2A_1 \cosh_{(K,\frac{-5}{3})}(-3\Gamma t) \tag{8}$$

and

$$\Delta = 2A_2 \cosh_{(K,-2)}(-2\Gamma t) \tag{9}$$

It is worth noting that, for $s = 1$ in Equation (7), the Rabi frequency is given by Arai's q-deformed waveform function (See Figure 2). This asymmetric pulse was investigated in three-level atoms to control the optical properties of the system in [23].

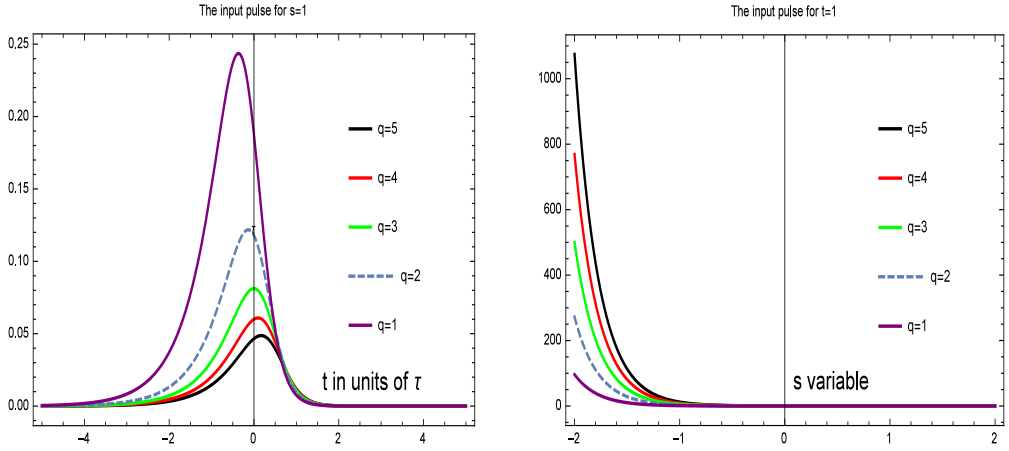

Figure 2. The pulse dynamics.

To determine the solutions of Equation (4), we consider three new variables, v_1, u_1 and w_1, linked to the previous variables $u(t)$, $v(t)$, and $w(t)$ as:

$$v_1(t) = v(t)e^{\Gamma t} \tag{10}$$
$$u_1(t) = u(t)e^{\Gamma t} \tag{11}$$
$$w_1(t) = w(t)e^{\Gamma t} \tag{12}$$

In addition, by means of a new change of variables $x = \int \Delta(t)dt$, and considering $g(x) = \frac{\Omega(x)}{\Delta(x)}$ and $h(x) = \frac{\Gamma}{\Delta(x)}$, Equation (4) gives:

$$\frac{du_1}{dx} = -v_1(x) \tag{13}$$

$$\frac{dv_1}{dx} = u_1(x) - g(x)w_1(x) \tag{14}$$

$$\frac{dw_1}{dx} = h(x)w_1(x) + g(x)v_1(x) \tag{15}$$

This system of differential equations will serve as a basis for our analysis to establish the exact solutions for the considered pulse. The variable $x(t)$ is defined as:

$$x(t) = (1 + Ke^{-2\Gamma t})^2 \tag{16}$$

We obtain the following ordinary differential equations by repetitive differentiation and substitution of the Equations (13)–(15).

$$\frac{d^3u_1(x)}{dx^3} + \sqrt{x}\frac{du_1(x)}{dx} = 0 \tag{17}$$

$$v_1(x) = -\frac{du_1(x)}{dx} \tag{18}$$

$$w(x) = u_1(x) + \frac{d^2u_1(x)}{dx^2} \tag{19}$$

To solve Equation (17), we let $U_1 = \frac{du_1(x)}{dx}$, then we obtain a second-order linear differential equation

$$\frac{d^2U_1(x)}{dx^2} + \sqrt{x}U_1(x) = 0$$

which has a solution given by

$$U_1(x) = c_1\sqrt{x}J_{\frac{2}{5}}\left(\frac{4}{5}x^{\frac{5}{4}}\right) + c_2\sqrt{x}Y_{\frac{2}{5}}\left(\frac{4}{5}x^{\frac{5}{4}}\right)$$

where c_1, c_2 are constants and $J_\nu(x), Y_\nu(x)$, are, respectively, the Bessel function of the first kind and the Bessel function of the second kind. Integrating $U_1(x)$ leads to $u_1(x)$. Then, by taking the derivatives of $u_1(x)$ and using Equations (18) and (19), we obtain $v_1(x)$ and $w(x)$.

4. Results and Discussion

Using the following initial conditions, we can determine the exact expressions of the coherence and population inversion: $u(0) = 2\sqrt{A(1-A)}$, $v(0) = 0$, $w(0) = 1 - 2A$ where $0 < A < 1$.

$$\begin{aligned} u_1(x) \quad = \quad & -\frac{8}{25}x^{\frac{5}{4}}S\left(-\frac{4}{5}, \frac{3}{5}, \frac{4}{5}x^{\frac{5}{4}}\right)\left[c_2J_{\frac{2}{5}}\left(\frac{4}{5}x^{\frac{5}{4}}\right) + c_3Y_{\frac{2}{5}}\left(\frac{4}{5}x^{\frac{5}{4}}\right)\right] - \\ & \frac{4}{5}x^{\frac{5}{4}}S\left(\frac{1}{5}, \frac{2}{5}, \frac{4}{5}x^{\frac{5}{4}}\right)\left[c_2J_{-\frac{3}{5}}\left(\frac{4}{5}x^{\frac{5}{4}}\right) + c_3Y_{-\frac{3}{5}}\left(\frac{4}{5}x^{\frac{5}{4}}\right)\right] \end{aligned} \tag{20}$$

$$\begin{aligned} v_1(x) \quad = \quad & -\frac{48}{125}x^{\frac{3}{2}}\left[c_2J_{\frac{2}{5}}\left(\frac{4}{5}x^{\frac{5}{4}}\right) + c_3Y_{\frac{2}{5}}\left(\frac{4}{5}x^{\frac{5}{4}}\right)\right] \times \\ & \left[S\left(\frac{-9}{5}, \frac{2}{5}, \frac{4}{5}x^{\frac{5}{4}}\right) + \frac{25}{12}S\left(\frac{1}{5}, \frac{2}{5}, \frac{4}{5}x^{\frac{5}{4}}\right)\right] \end{aligned} \tag{21}$$

$$
\begin{aligned}
w(x) \;=\; & -\frac{1}{25x^{\frac{3}{4}}}\Bigg[\Bigg(-10c_2J_{\frac{2}{5}}\left(\frac{4}{5}x^{\frac{5}{4}}\right)x^{\frac{5}{4}}-10c_3Y_{\frac{2}{5}}\left(\frac{4}{5}x^{\frac{5}{4}}\right)x^{\frac{5}{4}}+ \\
& 4(5x^2-5x^{\frac{5}{2}})\left(c_2J_{\frac{-3}{5}}\left(\frac{4}{5}x^{\frac{5}{4}}\right)+c_3Y_{\frac{-3}{5}}\left(\frac{4}{5}x^{\frac{5}{4}}\right)\right)\Bigg)S\left(\frac{1}{5},\frac{2}{5},\frac{4}{5}x^{\frac{5}{4}}\right)+ \\
& \Bigg(\frac{-24}{5}c_2J_{\frac{2}{5}}\left(\frac{4}{5}x^{\frac{5}{4}}\right)x^{\frac{5}{4}}-\frac{24}{5}c_3Y_{\frac{2}{5}}\left(\frac{4}{5}x^{\frac{5}{4}}\right)x^{\frac{5}{4}}- \\
& \frac{48}{5}x^{\frac{5}{2}}\left(c_2J_{\frac{-3}{5}}\left(\frac{4}{5}x^{\frac{5}{4}}\right)+c_3Y_{\frac{-3}{5}}\left(\frac{4}{5}x^{\frac{5}{4}}\right)\right)\Bigg)S\left(\frac{-9}{5},\frac{2}{5},\frac{4}{5}x^{\frac{5}{4}}\right)+ \\
& (8x^2+8x^{\frac{5}{2}})\left(c_2J_{\frac{2}{5}}\left(\frac{4}{5}x^{\frac{5}{4}}\right)+c_3Y_{\frac{2}{5}}\left(\frac{4}{5}x^{\frac{5}{4}}\right)\right)S\left(\frac{-4}{5},\frac{3}{5},\frac{4}{5}x^{\frac{5}{4}}\right)+ \\
& \frac{576}{25}\left(c_2J_{\frac{2}{5}}\left(\frac{4}{5}x^{\frac{5}{4}}\right)\right)+c_3Y_{\frac{2}{5}}\left(\frac{4}{5}x^{\frac{5}{4}}\right)\Bigg)S\left(\frac{-14}{5},\frac{3}{5},\frac{4}{5}x^{\frac{5}{4}}\right)-25c_1x^{\frac{3}{4}}\Bigg]
\end{aligned}
\tag{22}
$$

where $J_\nu(x), Y_\nu(x)$, $S(\nu,\mu,x)$ are, respectively, the Bessel function of the first kind, the Bessel function of the second kind, and the Lommel function and c_1, c_2 and c_3 are constants defined as follows

$$
c_1 = -\frac{50A\;S\left(\frac{1}{5},\frac{2}{5},\frac{4}{5}\right)-24S\left(\frac{-9}{5},\frac{2}{5},\frac{4}{5}\right)\sqrt{A(1-A)}-25S\left(\frac{1}{5},\frac{2}{5},\frac{4}{5}\right)}{12S\left(\frac{-9}{5},\frac{2}{5},\frac{4}{5}\right)+25S\left(\frac{1}{5},\frac{2}{5},\frac{4}{5}\right)} \tag{23}
$$

$$
c_2 = \frac{125\left(2A-1+2\sqrt{A(1-A)}\right)Y_{\frac{2}{5}}\left(\frac{4}{5}\right)}{4\left[J_{\frac{2}{5}}\left(\frac{4}{5}\right)Y_{\frac{-3}{5}}\left(\frac{4}{5}\right)-Y_{\frac{2}{5}}\left(\frac{4}{5}\right)J_{\frac{-3}{5}}\left(\frac{4}{5}\right)\right]\left[12S\left(\frac{-9}{5},\frac{2}{5},\frac{4}{5}\right)+25S\left(\frac{1}{5},\frac{2}{5},\frac{4}{5}\right)\right]} \tag{24}
$$

$$
c_3 = -\frac{125\left(2A-1+2\sqrt{A(1-A)}\right)J_{\frac{2}{5}}\left(\frac{4}{5}\right)}{4\left[J_{\frac{2}{5}}\left(\frac{4}{5}\right)Y_{\frac{-3}{5}}\left(\frac{4}{5}\right)-Y_{\frac{2}{5}}\left(\frac{4}{5}\right)J_{\frac{-3}{5}}\left(\frac{4}{5}\right)\right]\left[12S\left(\frac{-9}{5},\frac{2}{5},\frac{4}{5}\right)+25S\left(\frac{1}{5},\frac{2}{5},\frac{4}{5}\right)\right]} \tag{25}
$$

Therefore, the expressions of the real and imaginary parts of the coherence are given by:

$$
\begin{aligned}
u(t) \;=\; & -\frac{1}{5}\Bigg[\left(4S\left(\frac{1}{5},\frac{2}{5},\frac{4}{5}(1+Ke^{-2\Gamma t})^{\frac{5}{2}}\right)\left(c_2J_{-\frac{3}{5}}\left(\frac{4}{5}(1+Ke^{-2\Gamma t})^{\frac{5}{2}}\right)+\right.\right. \\
& \left.c_3Y_{-\frac{3}{5}}\left(\frac{4}{5}(1+Ke^{-2\Gamma t})^{\frac{5}{2}}\right)\right)+\frac{4}{5}\Bigg(2c_2J_{\frac{2}{5}}\left(\frac{4}{5}(1+Ke^{-2\Gamma t})^{\frac{5}{2}}\right)+ \\
& \left.2c_3Y_{\frac{2}{5}}\left(\frac{4}{5}(1+Ke^{-2\Gamma t})^{\frac{5}{2}}\right)\Bigg)S\left(-\frac{4}{5},\frac{3}{5},\frac{4}{5}\left(1+Ke^{-2\Gamma t}\right)^{\frac{5}{2}}\right)\right)(1+Ke^{-2\Gamma t})^{\frac{5}{2}}e^{-\Gamma t}\Bigg]
\end{aligned}
\tag{26}
$$

and

$$
\begin{aligned}
v(t) \;=\; & -\frac{1}{125}\Bigg[\left(144Ke^{-2\Gamma t}+48Ke^{-6\Gamma t}+144Ke^{-4\Gamma t}+48\right)\left(c_2J_{\frac{2}{5}}\left(\frac{4}{5}(1+Ke^{-2\Gamma t})^{\frac{5}{2}}\right)+\right. \\
& \left.c_3Y_{\frac{2}{5}}\left(\frac{4}{5}(1+Ke^{-2\Gamma t})^{\frac{5}{2}}\right)\right)e^{-\Gamma t}\left(S\left(\frac{-9}{5},\frac{2}{5},\frac{4}{5}(1+Ke^{-2\Gamma t})^{\frac{5}{2}}\right)+\frac{25}{12}S\left(\frac{1}{5},\frac{2}{5},\frac{4}{5}(1+Ke^{-2\Gamma t})^{\frac{5}{2}}\right)\right)\Bigg]
\end{aligned}
\tag{27}
$$

and the time evolution of the atomic population inversion as:

$$
\begin{aligned}
w(t) \;=\; & \frac{1}{125\sqrt{1+Ke^{-2\Gamma t}}}\Bigg[24\Bigg(\Bigg((1+Ke^{-2\Gamma t})^{\frac{3}{2}}c_2 J_{\frac{2}{5}}\Big(\frac{4}{5}(1+Ke^{-2\Gamma t})^{\frac{5}{2}}\Big)+ \\
& (1+Ke^{-2\Gamma t})^{\frac{3}{2}}c_3 Y_{\frac{2}{5}}\Big(\frac{4}{5}(1+Ke^{-2\Gamma t})^{\frac{5}{2}}\Big)+8\Big(Ke^{-2\Gamma t}+\frac{1}{4}Ke^{-8\Gamma t}+Ke^{-6\Gamma t}+\frac{3}{2}Ke^{-4\Gamma t}+\frac{1}{4}\Big) \\
& \Big(c_2 J_{\frac{-3}{5}}\Big(\frac{4}{5}(1+Ke^{-2\Gamma t})^{\frac{5}{2}}\Big)+c_3 Y_{\frac{-3}{5}}\Big(\frac{4}{5}(1+Ke^{-2\Gamma t})^{\frac{5}{2}}\Big)\Big)\Bigg)S\Big(\frac{-9}{5},\frac{2}{5},\frac{4}{5}(1+Ke^{-2\Gamma t})^{\frac{5}{2}}\Big)+ \\
& \Big(\frac{25}{12}(1+Ke^{-2\Gamma t})^{\frac{3}{2}}c_2 J_{\frac{2}{5}}\Big(\frac{4}{5}(1+Ke^{-2\Gamma t})^{\frac{5}{2}}\Big)\Big)+\frac{25}{12}(1+Ke^{-2\Gamma t})^{\frac{3}{2}}c_3 Y_{\frac{2}{5}}\Big(\frac{4}{5}(1+Ke^{-2\Gamma t})^{\frac{5}{2}}\Big)+ \\
& \frac{1}{6}\Bigg(25\Bigg(c_2 J_{\frac{-3}{5}}\Big(\frac{4}{5}(1+Ke^{-2\Gamma t})^{\frac{5}{2}}\Big)+c_3 Y_{\frac{-3}{5}}\Big(\frac{4}{5}(1+Ke^{-2\Gamma t})^{\frac{5}{2}}\Big) \\
& \big(Ke^{-2\Gamma t}+Ke^{-8\Gamma t}+3Ke^{-6\Gamma t}+3Ke^{-4\Gamma t}\big)\Bigg)\Bigg)S\Big(\frac{1}{5},\frac{2}{5},\frac{4}{5}(1+Ke^{-2\Gamma t})^{\frac{5}{2}}\Big)- \\
& \frac{1}{5}\Bigg(96\Big(Ke^{-2\Gamma t}+\frac{1}{4}Ke^{-8\Gamma t}+Ke^{-6\Gamma t}+\frac{3}{2}Ke^{-4\Gamma t}+\frac{1}{4}\Big) \\
& \Big(c_2 J_{\frac{2}{5}}\Big(\frac{4}{5}(1+Ke^{-2\Gamma t})^{\frac{5}{2}}\Big)+c_3 Y_{\frac{2}{5}}\Big(\frac{4}{5}(1+Ke^{-2\Gamma t})^{\frac{5}{2}}\Big)\Big)S\Big(\frac{-14}{5},\frac{3}{5},\frac{4}{5}(1+Ke^{-2\Gamma t})^{\frac{5}{2}}\Big)- \\
& \frac{1}{3}\Bigg(35\Big(Ke^{-2\Gamma t}+\frac{1}{7}Ke^{-8\Gamma t}+\frac{5}{7}Ke^{-6\Gamma t}+\frac{9}{7}Ke^{-4\Gamma t}+\frac{2}{7}\Big) \\
& \Big(c_2 J_{\frac{2}{5}}\Big(\frac{4}{5}(1+Ke^{-2\Gamma t})^{\frac{5}{2}}\Big)+c_3 Y_{\frac{2}{5}}\Big(\frac{4}{5}(1+Ke^{-2\Gamma t})^{\frac{5}{2}}\Big)\Big)S\Big(\frac{-4}{5},\frac{3}{5},\frac{4}{5}(1+Ke^{-2\Gamma t})^{\frac{5}{2}}\Big)\Bigg)\Bigg) \\
& +\frac{125}{24}c_1\sqrt{1+Ke^{-2\Gamma t}}\Bigg)\Bigg]
\end{aligned}
\tag{28}
$$

At the steady state, we obtain:

$$
W(\infty)=\frac{\Big(24A-12+24\sqrt{A(1-A)}\Big)S\Big(\frac{-9}{5},\frac{2}{5},\frac{4}{5}\Big)}{12S\Big(\frac{-9}{5},\frac{2}{5},\frac{4}{5}\Big)+25S\Big(\frac{1}{5},\frac{2}{5},\frac{4}{5}\Big)} \tag{29}
$$

In the following, we consider that the time is normalized to the unit of $1/\Gamma$. A_1, A_2 are normalized to the unit of Γ. We plot our results in Figures 3–5. First, Figure 3 reports the temporal dynamics of u(t,A), which is a real part of the coherence in the system. This is interpreted as the dispersion profile of two-level atoms. A in the figure represents the initial atomic population in the ground state. For A = 0, the initial atomic population is assumed to be in the excited state (initially). For A $\neq$ 0, the initial atomic population is distributed among the ground and the excited state. We observe a switch from positive to negative in the dispersion profile. This happens whenever A switches from 0 to any positive value (i.e., from the atomic population being totally in the excited state initially, to the case where the atomic population is distributed between the ground and the excited state). In the transient regime, we notice that the dispersion is negative, it becomes positive after $t \geq 0.5$. Additionally, the peaks are more pronounced for bigger A. This means that the dispersion peak is enhanced if initially we have more atomic populations at the ground state.

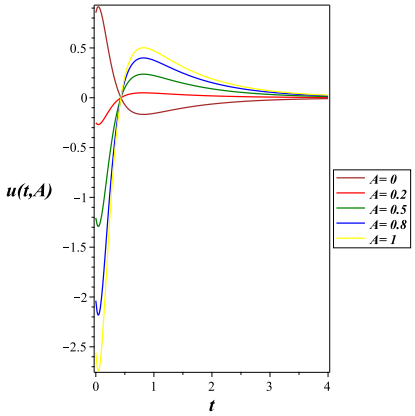

Figure 3. The real part of the coherence: related to the dispersion for $K = \Gamma = 1$.

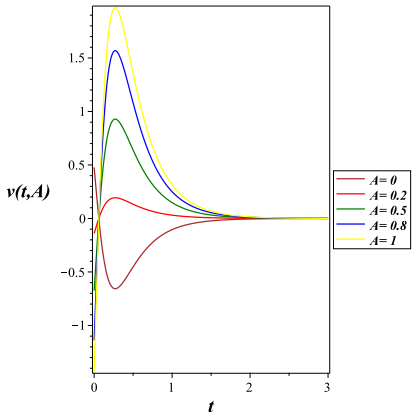

Figure 4. The imaginary part of the coherence: related to the absorption for $K = \Gamma = 1$.

Figure 4 shows the absorption profile of the two-level atom which is given by the imaginary part of the coherence. The absorption spectra are positive except for the case where the initial atomic population is considered to be fully at the excited state. Moreover, we observe that the highest peak is obtained for A = 1 where the initial atomic population is totally at the ground state. The peaks decrease as we consider the initial atomic populations distributed among the ground and the excited state.

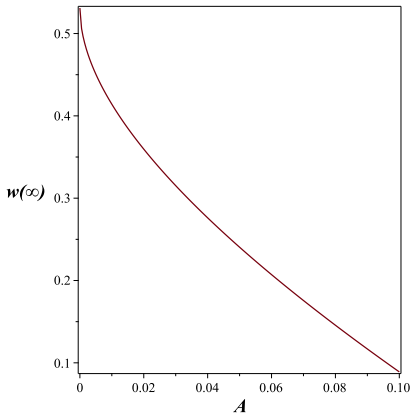

Figure 5. The atomic population inversion for $K = \Gamma = 1$.

Finally, Figure 5 reports the atomic population inversion at a large time (the infinity), for various values of A. We recall that A denotes the initial atomic population at the ground state. We clearly observe that the atomic population inversion at the steady state reaches

50% when the initial atomic population is considered to be totally in the ground state, whereas it decreases for greater values of A.

5. Conclusions

In this paper, we have derived the exact analytical solutions to the Bloch equations for a two-level atom with dephasing under chirped detuning. Our system is excited by an external asymmetric (generalized q-deformed) pulse, which couples the ground state to the excited state. We obtained full analytical solutions for the absorption and dispersion spectra (which are related to the real and imaginary parts of the coherence). Additionally, we determined the exact expression of the atomic population inversion at the steady state.

Author Contributions: Conceptualization, H.E.; Methodology, S.G. and H.E.; Validation, S.G.; Formal analysis, S.G. and N.B.; Investigation, S.G., N.B. and H.E.; Writing—original draft, S.G., N.B.; Writing—review and editing, H.E. All authors have read and agreed to the published version of the manuscript.

Funding: S. Grira acknowledges financial support from Abu Dhabi University's Office of Research and Sponsored Programs. Grant number: 19300651.

Institutional Review Board Statement: Not applicable.

Informed Consent Statement: Not applicable.

Data Availability Statement: Not applicable.

Conflicts of Interest: The authors declare no conflict of interest.

References

1. Bloch, F. Nuclear induction. *Phys. Rev.* **1946**, *70*, 460. [CrossRef]
2. Slobodeniuk, A.; Koutenskỳ, P.; Bartoš, M.; Trojánek, F.; Malỳ, P.; Novotnỳ, T.; Kozák, M. Semiconductor Bloch equation analysis of optical Stark and Bloch-Siegert shifts in monolayer WSe 2 and MoS 2. *Phys. Rev. B* **2022**, *106*, 235304. [CrossRef]
3. Boutabba, N. Kerr-effect analysis in a three-level negative index material under magneto cross-coupling. *J. Opt.* **2018**, *20*, 025102. [CrossRef]
4. Wendler, F.; Knorr, A.; Malic, E. Carrier multiplication in graphene under Landau quantization. *Nat. Commun.* **2014**, *5*, 3703. [CrossRef] [PubMed]
5. Liang, D.; Zhu, Y.; Li, H. Collective Resonance of D States in Rubidium Atoms Probed by Optical Two-Dimensional Coherent Spectroscopy. *Phys. Rev. Lett.* **2022**, *128*, 103601. [CrossRef] [PubMed]
6. Zlatanov, K.N.; Vitanov, N.V. Adiabatic generation of arbitrary coherent superpositions of two quantum states: Exact and approximate solutions. *Phys. Rev. A* **2017**, *96*, 013415. [CrossRef]
7. Schreiber, M.A.; Popp, J.; Seitner, L.; Haider, M.; Jirauschek, C. Implementation of Partially Reflecting Boundary Conditions in the Generalized Maxwell-Bloch Equations. In Proceedings of the 2022 International Conference on Numerical Simulation of Optoelectronic Devices (NUSOD), Turin, Italy, 12–16 September 2022; IEEE: Piscataway, NJ, USA, 2022; pp. 99–100.
8. Ossiander, M.; Golyari, K.; Scharl, K.; Lehnert, L.; Siegrist, F.; Bürger, J.; Zimin, D.; Gessner, J.; Weidman, M.; Floss, I.; et al. The speed limit of optoelectronics. *Nat. Commun.* **2022**, *13*, 1620. [CrossRef]
9. Allen, L.; Eberly, J.H. *Optical Resonance and Two-Level Atoms*; Courier Corporation: Chelmsford, MA, USA, 1975.
10. Letokhov, V.S. *Nonlinear Selective Photoprocesses in Atoms and Molecules*; Moscow Izdatel Nauka: Moscow, Russia, 1983.
11. Andreev, A.V.; Emel'yanov, V.I.; Il'inski, Y.A. Cooperative Phenomena in Optics. *Science* **1988**. Available online: https://catalog.loc.gov/vwebv/search?searchCode=LCCN&searchArg=88162206&searchType=1&permalink=y (accessed on 23 February 2023).
12. Singh, H.; Srivastava, H. Numerical simulation for fractional-order Bloch equation arising in nuclear magnetic resonance by using the Jacobi polynomials. *Appl. Sci.* **2020**, *10*, 2850. [CrossRef]
13. Reeves, L.; Shaw, K. Nuclear magnetic resonance studies of multi-site chemical exchange. I. Matrix formulation of the Bloch equations. *Can. J. Chem.* **1970**, *48*, 3641–3653. [CrossRef]
14. Xu, Z.; Zhou, Y.; Peng, X.; Li, L.; Qiu, X.; Zhou, M.; Xu, X. Measuring the enhancement factor of the hyperpolarized Xe in nuclear magnetic resonance gyroscopes. *Phys. Rev. A* **2021**, *103*, 023114. [CrossRef]
15. Xiao, W.; Wu, T.; Peng, X.; Guo, H. Atomic spin-exchange collisions in magnetic fields. *Phys. Rev. A* **2021**, *103*, 043116. [CrossRef]
16. Kocharovskaya, O.; Zhu, S.Y.; Scully, M.O.; Mandel, P.; Radeonychev, Y. Generalization of the Maxwell-Bloch equations to the case of strong atom-field coupling. *Phys. Rev. A* **1994**, *49*, 4928. [CrossRef] [PubMed]
17. Wein, S.C.; Loredo, J.C.; Maffei, M.; Hilaire, P.; Harouri, A.; Somaschi, N.; Lemaître, A.; Sagnes, I.; Lanco, L.; Krebs, O.; et al. Photon-number entanglement generated by sequential excitation of a two-level atom. *Nat. Photonics* **2022**, *16*, 374–379. [CrossRef]

18. Grira, S.; Boutabba, N.; Eleuch, H. Atomic population inversion in a two-level atom for shaped and chirped laser pulses: Exact solutions of Bloch equations with dephasing. *Results Phys.* **2021**, *26*, 104419. [CrossRef]
19. Devi, A.; Gunapala, S.D.; Premaratne, M. Coherent and incoherent laser pump on a five-level atom in a strongly coupled cavity-QED system. *Phys. Rev. A* **2022**, *105*, 013701. [CrossRef]
20. Boutabba, N.; Grira, S.; Eleuch, H. Atomic population inversion and absorption dispersion-spectra driven by modified double-exponential quotient pulses in a three-level atom. *Results Phys.* **2021**, *24*, 104108. [CrossRef]
21. Zlatanov, K.N.; Vasilev, G.S.; Ivanov, P.A.; Vitanov, N.V. Exact solution of the Bloch equations for the nonresonant exponential model in the presence of dephasing. *Phys. Rev. A* **2015**, *92*, 043404. [CrossRef]
22. Grira, S.; Boutabba, N.; Eleuch, H. Exact solutions of the Bloch equations of a two-level atom driven by the generalized double exponential quotient pulses with dephasing. *Mathematics* **2022**, *10*, 2105. [CrossRef]
23. Boutabba, N.; Grira, S.; Eleuch, H. Analysis of a q-deformed hyperbolic short laser pulse in a multi-level atomic system. *Sci. Rep.* **2022**, *12*, 9308. [CrossRef]
24. Zhang, J.; Garwood, M.; Park, J.Y. Full analytical solution of the bloch equation when using a hyperbolic-secant driving function. *Magn. Reson. Med.* **2017**, *77*, 1630–1638. [CrossRef] [PubMed]
25. Silver, M.; Joseph, R.; Hoult, D. Selective spin inversion in nuclear magnetic resonance and coherent optics through an exact solution of the Bloch-Riccati equation. *Phys. Rev. A* **1985**, *31*, 2753. [CrossRef] [PubMed]
26. Vasilev, G.; Ivanov, P.; Vitanov, N. Exact solution of the optical Bloch equation for the Demkov model. *arXiv* **2014**, arXiv:1402.5648.
27. Longmire, C.L.; Hamilton, R.M.; Hahn, J.M. *A Nominal Set of High-Altitude EMP Environments*; Technical Report; Mission Research Corp.: Santa Barbara, CA, USA; Oak Ridge National Lab.: Oak Ridge, TN, USA, 1987.
28. Pretzler, G.; Kasper, A.; Witte, K. Angular chirp and tilted light pulses in CPA lasers. *Appl. Phys. B* **2000**, *70*, 1–9. [CrossRef]
29. Wang, M.; Li, P.; Li, S.; Xu, Y.; Yao, C. Hundred-watt level average power CPA system with all-fiberized laser amplifiers based on CFBG stretcher and CVBG compressor. *Optik* **2022**, *253*, 168597. [CrossRef]
30. Roeder, S.; Zobus, Y.; Brabetz, C.; Bagnoud, V. How the laser beam size conditions the temporal contrast in pulse stretchers of chirped-pulse amplification lasers. *High Power Laser Sci. Eng.* **2022**, *10*, e34. [CrossRef]
31. Li, H.; MacArthur, J.; Littleton, S.; Dunne, M.; Huang, Z.; Zhu, D. Femtosecond-Terawatt Hard X-Ray Pulse Generation with Chirped Pulse Amplification on a Free Electron Laser. *Phys. Rev. Lett.* **2022**, *129*, 213901. [CrossRef]
32. Mao, D.; He, Z.; Zhang, Y.; Du, Y.; Zeng, C.; Yun, L.; Luo, Z.; Li, T.; Sun, Z.; Zhao, J. Phase-matching-induced near-chirp-free solitons in normal-dispersion fiber lasers. *Light Sci. Appl.* **2022**, *11*, 25. [CrossRef]
33. Ghotra, H.S. Laser wakefield and direct laser acceleration of electron by chirped laser pulses. *Optik* **2022**, *260*, 169080. [CrossRef]
34. Meystre, P.; Scully, M.O. *Quantum Optics*; Springer: Berlin/Heidelberg, Germany, 2021.
35. Rogovin, D.; Scully, M.O. Does the "two-level atom" picture of a josephson junction have a theoretical foundation in BCS? *Ann. Phys.* **1974**, *88*, 371–396. [CrossRef]
36. Jabri, H.; Eleuch, H. Enhanced unconventional photon-blockade effect in one-and two-qubit cavities interacting with nonclassical light. *Phys. Rev. A* **2022**, *106*, 023704. [CrossRef]
37. Zhao, C.; Peng, R.; Yang, Z.; Chao, S.; Li, C.; Zhou, L. Atom-Mediated Phonon Blockade and Controlled-Z Gate in Superconducting Circuit System. *Ann. Phys.* **2021**, *533*, 2100039. [CrossRef]
38. Glushkov, A.V. *Relativistic Quantum Theory. Quantum Mechanics of Atomic Systems*; Astroprint: Odessa, Ukraine, 2008.
39. Shore, B.W. The Theory of Coherent Atomic Excitation. In two volumes. Vol. 1, Simple Atoms and Fields. Vol. 2, Multilevel Atoms and Incoherence. *Science* **1990**, *250*, 1735.
40. Chollangi, A.; Ravi, Krishnan, N.; Bhowmick, K. An Investigation of Transmission Properties of Double-Exponential Pulses in Core-Clad Optical Fibers for Communication Application. In *Lecture Notes of the Institute for Computer Sciences, Social Informatics and Telecommunications Engineering*; Springer International Publishing: Cham, Switzerland, 2019; Volume 276.
41. Chollangi, A.; Thakur, A.K.; Rakesh, R.; Alharbi, S.; Bhowmick, K. Investigation of transmission properties of a practical double exponential pulse for communication and sensing application. *Optik* **2022**, *255*, 168735. [CrossRef]
42. Arkhipov, M.V.; Arkhipov, R.M.; Pakhomov, A.V.; Babushkin, I.V.; Demircan, A.; Morgner, U.; Rosanov, N.N. Generation of unipolar half-cycle pulses via unusual reflection of a single-cycle pulse from an optically thin metallic or dielectric layer. *Opt. Lett.* **2017**, *42*, 2189–2192. [CrossRef] [PubMed]
43. Arkhipov, R.; Arkhipov, M.; Pakhomov, A.; Babushkin, I.; Rosanov, N. Half-cycle and unipolar pulses (Topical Review). *Laser Phys. Lett.* **2022**, *19*, 043001. [CrossRef]
44. Morrow, D.J.; Ma, X. Rapid and facile reconstruction of time-resolved fluorescence data with exponentially modified Gaussians. *Opt. Open* 2022, *preprint*.
45. Abdalla, M.S.; Eleuch, H. Exact analytic solutions of the Schrödinger equations for some modified q-deformed potentials. *J. Appl. Phys.* **2014**, *115*, 234906. [CrossRef]